

# Effect of Curvature on the Neutral Stability Boundary for Cellular Gaseous Detonations

Mark Short, Stephen J. Voelkel, Carlos Chiquete  
Shock and Detonation Physics, Los Alamos National Laboratory,  
Los Alamos, NM 87544, USA

## 1 Introduction

For one-step Arrhenius reactions, a significant volume of work has been conducted on establishing the neutral stability boundaries for two-dimensional cellular instabilities to develop from a one-dimensional Zeldovich-von Neumann-Döring wave (ZND) structure in rigid channels [1–3]. In the one-step model, for fixed ratio of specific heats ( $\gamma$ ), these boundaries are characterized by variations in the heat release ( $Q$ ) and activation energy ( $E$ ), as shown in Fig 1. For large activation energies, very small values of the heat release lead to the ZND wave becoming unstable to two-dimensional perturbations, while for lower activation energies a larger heat release is required. Establishing the neutral stability boundaries has proven important for understanding some of the mechanisms of cellular detonation onset [1–3]. Although the 1D steady ZND solution does not depend on the channel width, the cellular structure does, particularly for narrow channels in which mode-locking can occur [2, 4].

What has not been studied to date is how this neutral stability boundary is affected when the reference steady wave is curved. Such bulk curvature can be induced in a number of ways, for example by having yielding confinement at the boundary, e.g., with an inert gas lying outside the reactive gas [5–8]. With yielding confinement, the flow behind the shock expands laterally. This causes the shock to become divergently curved, and, in response, the flow sonic plane moves into regions of incomplete reaction [9–11]. For the steady curved detonation construct, the region between the detonation shock and sonic plane is known as the detonation driving zone (or DDZ) [11]. As the width of the reactive gas layer is decreased, the steady axial detonation speed decreases, creating a diameter effect curve [12]. Note that such DDZ solutions cannot be constructed analytically. However, the structure of the steady curved detonation wave now not only depends on  $\gamma$ ,  $Q$ , and  $E$ , but also on the width of the channel and the degree of confinement. Both of the latter two factors influence the amount of curvature that can be induced on the detonation front.

In Chiquete *et al.* [12], we examined the effect of the degree of confinement on detonation cell structure for a one-step Arrhenius reaction. As the degree of confinement is reduced, the number of cells initially grows for a fixed channel width and then decreases. Eventually, for certain channel sizes, a steady (non-cellular) wave is recovered for sufficiently weak confinement. This indicates that bulk curvature can cause a detonation wave that is cellular in a rigid channel to cross a neutral stability boundary as the confinement is reduced. Mi *et al.* [13] and Reynaud *et al.* [14] both report cases where, for a sufficiently

narrow explosive layer with yielding inert gas confinement, hydrodynamically stable curved fronts may be found. In both of these studies, the inert confining material had identical properties to that of the explosive, except reaction is turned off. Thus, the degree of confinement is difficult to establish as the shock polars are the same.

In the current study, we examine the shift in the rigid channel neutral stability boundary that occurs when semi-confined flows are considered. Specifically, we consider an inert bounding mixture that is not confining for the detonation, i.e., in a steady flow, the flow at the inert boundary is sonic. Then, for a fixed channel width and heat release, we reduce the activation energy until the detonation becomes stable with a well-defined DDZ structure. We examine the shift in the neutral stability boundary for multiple channel widths. In the limit of large channel widths, we expect to recover the rigid channel stability boundary.

## 2 Model, Geometry and Computational Methods

For the numerical simulations, the flow in the gaseous explosive is modeled with the reactive Euler equations

$$\frac{D\rho}{Dt} + \rho \nabla \cdot \mathbf{u} = 0, \quad \frac{D\mathbf{u}}{Dt} = -\frac{1}{\rho} \nabla p, \quad \frac{De}{Dt} = \frac{p}{\rho^2} \frac{D\rho}{Dt}, \quad (1)$$

for non-dimensional density  $\rho$ , pressure  $p$ , particle velocity  $\mathbf{u}$  and specific internal energy  $e$ . We use an ideal equation-of-state and assume a one-step Arrhenius chemical reaction,

$$e = \frac{p}{(\gamma - 1)\rho} - Q\lambda, \quad T = \frac{p}{\rho}, \quad \frac{D\lambda}{Dt} = k(1 - \lambda)e^{-E/T}, \quad (2)$$

where  $T$  is the temperature,  $\gamma$  is the adiabatic exponent,  $Q$  is the specific reaction enthalpy of the fuel species and  $E$  is the activation energy. Also,  $\lambda \in [0, 1]$  is the reaction progress. The non-dimensionalization is given by

$$p = \frac{\tilde{p}}{\tilde{p}_0}, \quad \rho = \frac{\tilde{\rho}}{\tilde{\rho}_0}, \quad \mathbf{u} = \frac{\tilde{\mathbf{u}}}{\sqrt{\tilde{p}_0/\tilde{\rho}_0}}, \quad e = \frac{\tilde{e}}{\tilde{p}_0/\tilde{\rho}_0}, \quad Q = \frac{\tilde{Q}}{\tilde{p}_0/\tilde{\rho}_0}, \quad E = \frac{\tilde{E}}{\tilde{p}_0/\tilde{\rho}_0}, \quad (3)$$

where the subscript  $\{ \}_0$  represents the quiescent reactant state. Length is scaled by  $\tilde{l}_{1/2}$ , the half-reaction zone length of the Zeldovich-von Neumann-Döring (ZND) detonation, and time ( $t$ ) by  $\tilde{l}_{1/2}/\sqrt{\tilde{p}_0/\tilde{\rho}_0}$ .

The geometry consists of a rectangular reactive gas region with width  $W$  and length  $L$ . In the calculations below,  $\gamma = 1.2$ , and  $E$ ,  $Q$  and  $W$  are varied. A rectangular inert confiner layer lies on top of the explosive region, having width  $W_i = 30$ . The subscript  $\{ \}_i$  refers to properties of the confiner material. Outflow conditions are applied to the top of the confiner boundary, with reflection conditions on the lower explosive boundary. The confiner is modeled with an ideal equation of state with  $\gamma_i = 1.2$ , along with an initial confiner density  $\rho_{0i} = 1$  and pressure  $p_{0i} = 0.1$ . Through shock polar analysis, it can be shown that for all the cases presented below, the inert layer does not confine the steady detonation structure in the reactive layer, i.e. the flow at intersection of the detonation shock with the inert boundary is sonic.

We use a modified form of the shock-fitted, shock-attached computational strategy described in [15]. The shock for the reactive and inert materials are mapped to the right-hand boundary in a Cartesian frame. The flow equations are integrated with a cell-centered finite volume method on a fixed, Cartesian mesh. A second-order centered-minmod reconstruction with a Lax-Friedrichs flux and second-order TVD Runge-Kutta integration are employed for spatial and temporal integration. The detonation and inert shock speeds and states are solved with the approach in [15]. We use a resolution of 10 or 20 points per the unit half-reaction-zone length. The initial conditions consist of a 1D ZND wave structure imposed across the explosive channel, slightly angled toward the inert confiner.

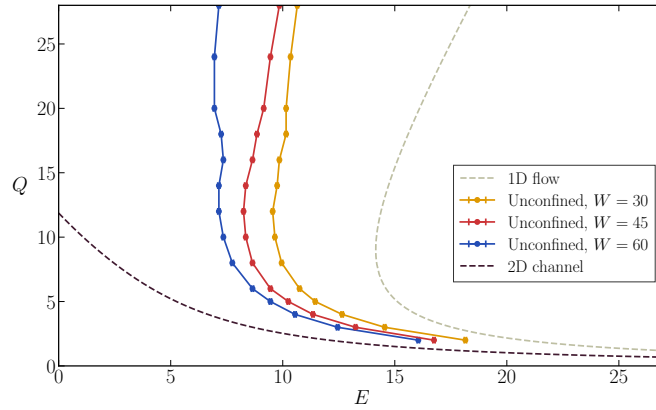


Figure 1: 2D neutral stability boundaries in  $(Q, E)$  space for unconfined channel flow for  $W = 30$ , 45, and 60. Also shown is the 2D neutral boundary for rigid channel flow, and the 1D flow neutral stability [3].

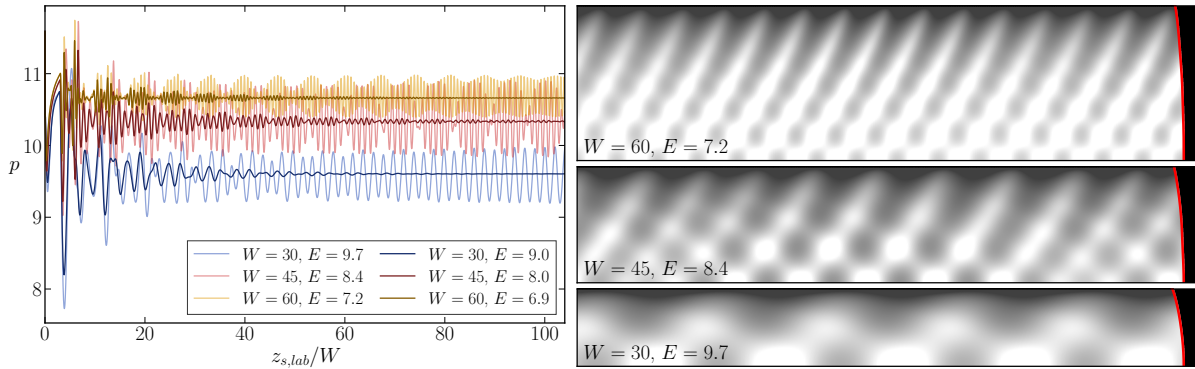


Figure 2: Left (L): Evolution of the detonation shock pressure in time along the rigid wall for various  $E$  cases either side of the neutral stability boundaries for  $Q = 12$ , and for each of the channel widths examined ( $W = 30, 45$ , and 60). Right (R): Pressure-based soot foil record for each of the unstable cases.

### 3 Stability Boundaries

Figure 1 shows the 2D neutral stability boundary for fully confined, rigid channels for  $\gamma = 1.2$  and varying  $Q$  and  $E$ . as well as that for 1D pulsating flow. The newly calculated 2D neutral stability boundaries in  $(Q, E)$  space for unconfined channel flow for  $W = 30, 45$ , and 60 lie between the 1D and 2D boundary for rigid channels. As the channel width increases, the boundary shifts to the left, i.e. for fixed  $Q$ , a smaller  $E$  generates 2D unstable flow. For large  $E$ , the curves converge. For smaller  $E$ , the effects of curvature are so dominant that cellular instabilities are prevented from forming for the range of  $Q$  shown.

Figure 2 shows the evolution of the detonation shock pressure in time along the lower rigid wall for various  $E$  cases either side of the neutral stability boundaries for  $Q = 12$ , and for each of the channel widths examined,  $W = 30, 45$ , and 60. For low enough  $E$ , the 2D perturbation to the detonation front decays in time, limiting to a hydrodynamically stable wave with no cells. The shock pressure-based soot foils shown in Fig. 2 illustrate that the front structure is very asymmetric for all  $W$  cases, with detonation cells forming near the rigid lower boundary, and the transverse wave propagating upward toward the

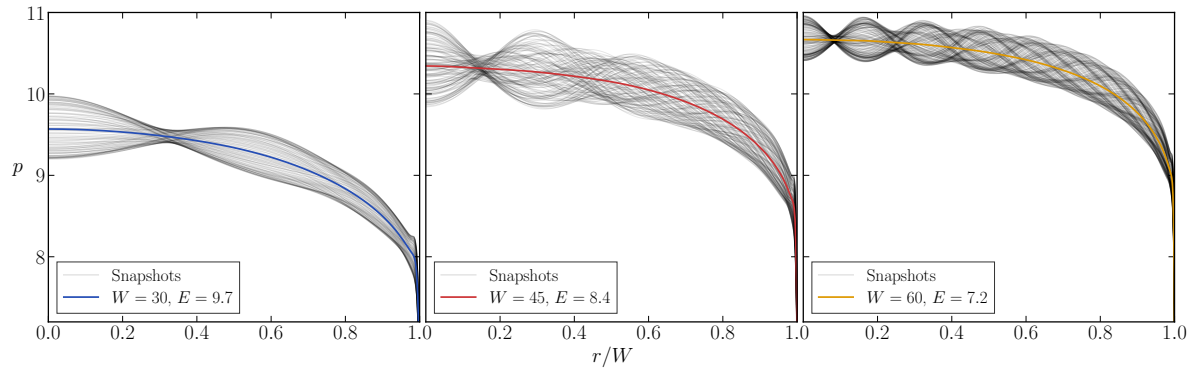


Figure 3: Sequence of shock pressure snapshots in time along the channel during the cellular evolution for the unstable cases in Fig. 2 for  $W = 30, 45,$  and  $60$ .

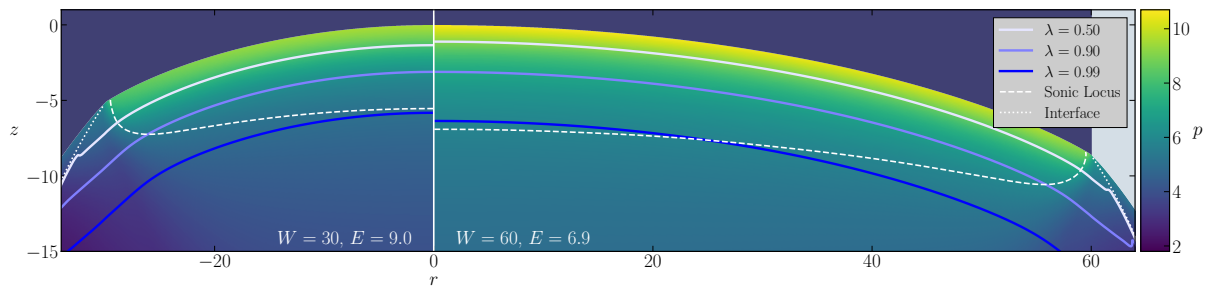


Figure 4: Detonation driving zone structure for the 2D stable cases shown in Fig. 2 for  $W = 30$  ( $E = 9.0$ ) and  $W = 60$  ( $E = 6.9$ ).

unconfined boundary without a strong counter propagating transverse wave [12]. The sequence of shock pressure snapshots in time along the channel shown in Fig. 3 during the cellular evolution for the unstable cases in Fig. 2 illustrate the nature of this asymmetry. The patterns, however, show the formation of regular, repeating structures. Figure 4 shows the detonation driving zone structure for the 2D stable cases shown in Fig. 2 for  $W = 30$  ( $E = 9.0$ ) and  $W = 60$  ( $E = 6.9$ ). They show the classic structure for unconfined flow, with a detonation shock, sonic locus internal to the reaction zone, and intersection of the detonation shock and sonic locus at the inert material boundary.

## 4 Summary

Curved detonations have been shown to have a significant effect on the neutral stability boundary for cellular flows. Moving forward, we will explore a wider range of channel widths to more fully map out the stability boundary for curved waves.

## References

- [1] J.J. Erpenbeck. Stability of idealized one-reaction detonations. *Phys. Fluids*, 7:684–696, 1964.
- [2] A. Bourlioux and A.J. Majda. Theoretical and numerical structure for unstable two-dimensional detonations. *Combust. Flame*, 90:211–229, 1992.

- 
- [3] M. Short and D.S. Stewart. Cellular detonation stability. part 1. a normal-mode linear analysis. *J. Fluid Mech.*, 368:229–262, 1998.
- [4] G.J. Sharpe. Transverse waves in numerical simulations of cellular detonations. *J. Fluid Mech.*, 447:31–51, 2001.
- [5] M. Monwar, K. Ishii, and T. Tsuboi. A study of propagating detonation waves in narrow channels. *J. Combust. Soc. Japan*, 51:334–342, 2009.
- [6] W. Rudy, M. Kuznetsov, R. Porowski, A. Teodorczyk, J. Grune, and K. Sempert. Critical conditions of hydrogen-air in partially confined geometry. *Proc. Combust. Instit.*, 34:1965–1972, 2013.
- [7] W. Rudy, M. Zbikowski, and A. Teodorczyk. Detonation in hydrogen-methane-air mixtures in semi-confined flat channels. *Energy*, 116:1479–1483, 2016.
- [8] J. Grune, K. Sempert, A. Friedrich, M. Kuznetsov, and T. Jordan. Detonation wave propagation in semi-confined layers of hydrogen-air and hydrogen-oxygen mixtures. *Int. J. Hydrogen Energy*, 42:7589–7599, 2017.
- [9] J.B. Bdzil. Steady-state two-dimensional detonation. *J. Fluid Mech.*, 108:195–226, 1981.
- [10] G.J. Sharpe and M. Braithwaite. Steady non-ideal detonations in cylindrical sticks of explosives. *J. Eng. Math.*, 53(1):39–58, 2005.
- [11] M. Short and J.J. Quirk. High explosive detonation-confiner interactions. *Annu. Rev. Fluid Mech.*, 50:215–242, 2018.
- [12] C. Chiquete, M. Short, and J.J. Quirk. The effect of curvature and confinement on gas-phase detonation cellular stability. *Proc. Combust. Instit.*, 37:3565–3573, 2019.
- [13] X. Mi, A.J. Higgins, H.D. Ng, C.B. Kiyanda, and N. Nikiforakis. Effect of spatial inhomogeneities on the propagation limit of gaseous detonations. In *26th ICDERS meeting, Boston, USA. 2017*.
- [14] M. Reynaud, F. Virost, and A. Chinnayya. Interactions of a detonation wave confined by a high-temperature compressible layer. In *26th ICDERS meeting, Boston, USA. 2017*.
- [15] C. Chiquete, M. Short, C.D. Meyer, and J.J. Quirk. Calibration of the pseudo-reaction-zone model for detonation wave propagation. *Combust. Theory Modell.*, 22:744–776, 2018.